iScience

CellPress
OPEN ACCESS

Article

Evaluation and projection of precipitation extremes under 1.5°C and 2.0°C GWLs over China using bias-corrected CMIP6 models

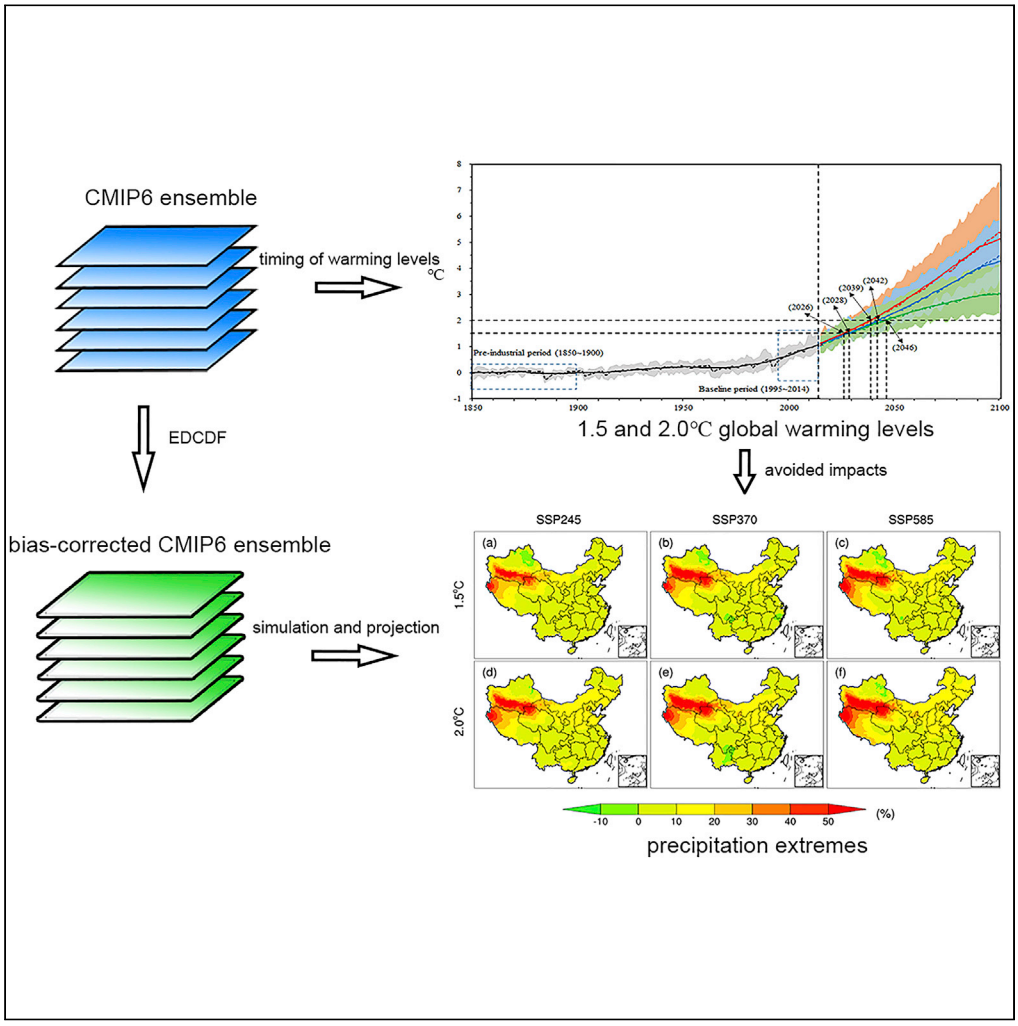

Junhong Guo, Yangshuo Shen, Xiuquan Wang, Xi Liang, Zhenlu Liu, Lvliu Liu

shenyangshuo@163.com

Highlights

Extreme precipitation will be more frequent and intense over China

Total precipitation changes attribute to an increase of very heavy precipitation

Limiting to 1.5°C and low emissions would have substantial benefits for China

Guo et al., iScience 26, 106179
April 21, 2023
https://doi.org/10.1016/j.isci.2023.106179

iScience

CellPress
OPEN ACCESS

Article

Evaluation and projection of precipitation extremes under 1.5°C and 2.0°C GWLs over China using bias-corrected CMIP6 models

Junhong Guo,[1] Yangshuo Shen,[2,6,*] Xiuquan Wang,[3] Xi Liang,[4] Zhenlu Liu,[1] and Lvliu Liu[5]

SUMMARY

China is facing an increasing challenge from severe precipitation-related extremes with accelerating global warming. In this study, using a bias-corrected CMIP6 ensemble, future responses of precipitation extreme indices at 1.5°C and 2.0°C global warming levels (GWLs) under the SSP245, SSP370 and SSP585 scenarios are investigated. Despite different change magnitudes, extreme precipitation events will be more frequent and more intense over China as a whole under higher emissions and GWLs. The increase in annual total precipitation could attribute to a sharp increase in the intensity and days of very heavy precipitation in future global warming scenarios. Limiting global warming to 1.5°C and low emission pathways (i.e., SSP245) instead of 2°C and high emission pathways (i.e., SSP585) would have substantial benefits for China in terms of reducing occurrences of extreme precipitation events.

INTRODUCTION

It has been widely accepted that the global mean temperature will continue to increase with the growing emissions of greenhouse gases.[1] Warming-induced changes exacerbate the variations in the occurrence of climate extremes in the aspect of duration, frequency, intensity, and spatial distribution.[2] The global water cycle patterns will be affected most probably by global warming. In particular, the precipitation-related serious consequences have an extensive impact on socioeconomic and ecological security.[3,4] According to the statistical results of the International Disaster Database,[5] in 2021, a total of 432 catastrophic events were recorded and floods dominated these events, with 223 occurrences, up from an average of 163 annual flood occurrences recorded across the 2001–2020 period. In July 2021, the Henan Flood in China was particularly severe, resulting in 352 deaths, 14.5 million people affected, and a cost of 16.5 billion US dollars. Therefore, a better understanding and detailed investigation of changes in global and regional extreme precipitation characteristics and their socioeconomic impacts in the 21st century should feed into long-term climate adaptation and mitigation plans for policymakers.

To meet the challenges of global warming, the Paris Agreement adopted in 2015 set the goal to hold "the increase in the global average temperature to well below 2°C above pre-industrial levels and to pursue efforts to limit the temperature increase to 1.5°C above pre-industrial levels".[6] Most countries began to plan climate actions based on the principle of "nationally determined contributions". In 2019, China has also proposed a plan of "double carbon targets", that is, reaching carbon peaking by 2030 and neutrality by 2060. However, China will still face considerable difficulties, such as adjustment of energy structure, the COVID-19 pandemic, etc. Although the policies have a continuous improvement for achieving these goals, there is a lack of scientific knowledge about the relative risks (i.e., extreme climate risks and their potential impacts) associated with the implications of 1.5°C and 2°C warming scenarios.[4]

Identifying regional climate features is an essential prerequisite for understanding their response to climate change. Quantifying global and regional climate at specific global warming levels (GWLs) has become widespread because this approach can isolate the uncertainty in the regional climate response from the global warming uncertainty induced by scenario, global mean model response and internal variability.[1] Climate models are one of the most popular tools to simulate past climatology and project future climate change. In terms of impact assessments of 1.5°C and 2°C GWLs, these models are classed into several types. One is called the warming targets model, which designs a near-equilibrium 1.5°C or 2°C

[1]MOE Key Laboratory of Resource and Environmental, System Optimization, College of Environmental Science and Engineering, North China Electric Power University, Beijing 102206, China

[2]School of Economics and Management, North China Electric Power University, Beijing 102206, China

[3]School of Climate Change and Adaptation, University of Prince Edward Island, Charlottetown, Prince Edward Island C1A 4P3, Canada

[4]Sustainable Finance and Infrastructure Transition, Bartlett School of Sustainable Construction, University College London, London WC1E 6BT, UK

[5]Beijing Climate Centre, China Meteorological Administration, Beijing, China

[6]Lead contact

*Correspondence: shenyangshuo@163.com

https://doi.org/10.1016/j.isci.2023.106179

warmer world and is produced by a coupled climate model (i.e., Community Earth System Model, CESM)[7] or multiple climate models (i.e., HAPPI model intercomparison project).[8,9] The second type is the transient simulations, which are based on the outputs of CMIP models. This way can evaluate the potential uncertainties from different emission scenarios (i.e., RCPs and SSPs).[10–15] Moreover, owing to more reasonable shared socioeconomic pathways (SSPs) by sharing policy assumptions, previous investigations showed that CMIP6 is more reliable and stable than CMIP5.[3] Over China, Yang et al., (2022)[16] employed 8 CMIP6 models to investigate temperature and precipitation changes in Northwest China under 5 SSP scenarios using the standardized precipitation evapotranspiration index. Based on the CMIP6 simulations, Zhu et al., (2021)[13] projected the changes in climate extremes over China under global warming of 1.5, 2.0 and 3.0°C above the pre-industrial period and proved that CMIP6 models outperform their predecessors in CMIP5. Likewise, Su et al., (2021)[17] used 4 CMIP6 models to analyze future drought characteristics over China under 7 SSP scenarios and conduct a comparison with CMIP5 for addressing the improvements added to CMIP6.

However, the substantial differences, especially in simulating precipitation, among CMIP models are likely because of differences in the forcings, the magnitude of the internal variability, and the climate sensitivity of individual models.[17] The range of these models may be too wide when unrealistic models are included or too narrow when models underestimate uncertainties from processes that are not or poorly represented.[18] Although the ensemble mean method is an effective way to reduce the uncertainty of independent models to some extent, the models with very high biases may still affect the whole performance of the ensemble. Therefore, climate impact studies need bias-corrected projections for decision makers at regional and local scales. Because the bias-corrected dataset is consistent with observation for a climatological mean period, it is easier to infer the project changes and their implications in different sectors (i.e., water resources and agriculture) for observations.[19]

In total, although the future changes in temperature and precipitation for China have been discussed previously, to the best of our knowledge, only a very few studies have been conducted to use CMIP6 data with bias correction to comprehensively visualize the future changes in the spatiotemporal distribution of extreme precipitation on the whole of China. Furthermore, because limiting global warming to 1.5°C might translate into substantial benefits, it is also significant to evaluate the reduction in risk if warming is limited to 1.5°C instead of 2°C above the pre-industrial level.

Therefore, the goals of this study are: (1) To evaluate the performance of the simulated extreme precipitation over China based on the bias-corrected CMIP6 models, (2) to project future changes in extreme precipitation indices over China under different SSPs scenarios, (3) to analyze the impacts on the extreme precipitation if the global warming is limited to 1.5°C rather than higher warming threshold of 2°C.

RESULTS

Model evaluation

The comparison before and after bias correction for the CMIP6 ensemble in simulating the precipitation extremes for the baseline period (1995–2014) over China is shown in Figures 1 and 2. The results show that the CMIP6 ensemble mean has reasonable skill in reproducing the annual total precipitation over China. Major precipitation centers (i.e., southeast) and dry regions (i.e., northwest) are simulated by the ensemble, though there is an artificial wet area simulated by the raw CMIP6 models over the southwest of China. Based on their relative biases between ensemble mean and observation CN05.1, it should be clear that the results through bias correction have an enormous improvement relative to the original models. Specifically, the raw CMIP6 ensemble has an obvious overestimation (even exceeding 80%) in the west of China, such as Tibet and the south of Xinjiang, but slight underestimation in the north of Xinjiang, nevertheless, these biases are removed totally through the bias correction and the overall corrected biases of annual total precipitation over China are keep in ~20% compared with the observation. In addition, worthy of note is that the lack of observed meteorological stations in the CN05.1 results in small precipitation in some regions (i.e., Taiwan) over China.

Likewise, the performance of after-corrected simulations in intensive and frequency precipitation extreme indices is better than the raw CMIP6 models. Overall, except for CWD, the largest errors are found in the west and the southern parts of Xinjiang and the east of China has smaller biases, particularly for the Rx5day. However, through the bias correction, some regions (i.e., the southwest of Xinjiang) show a sign of overcorrection, with an underestimation of ~60%. The biases in the southeast

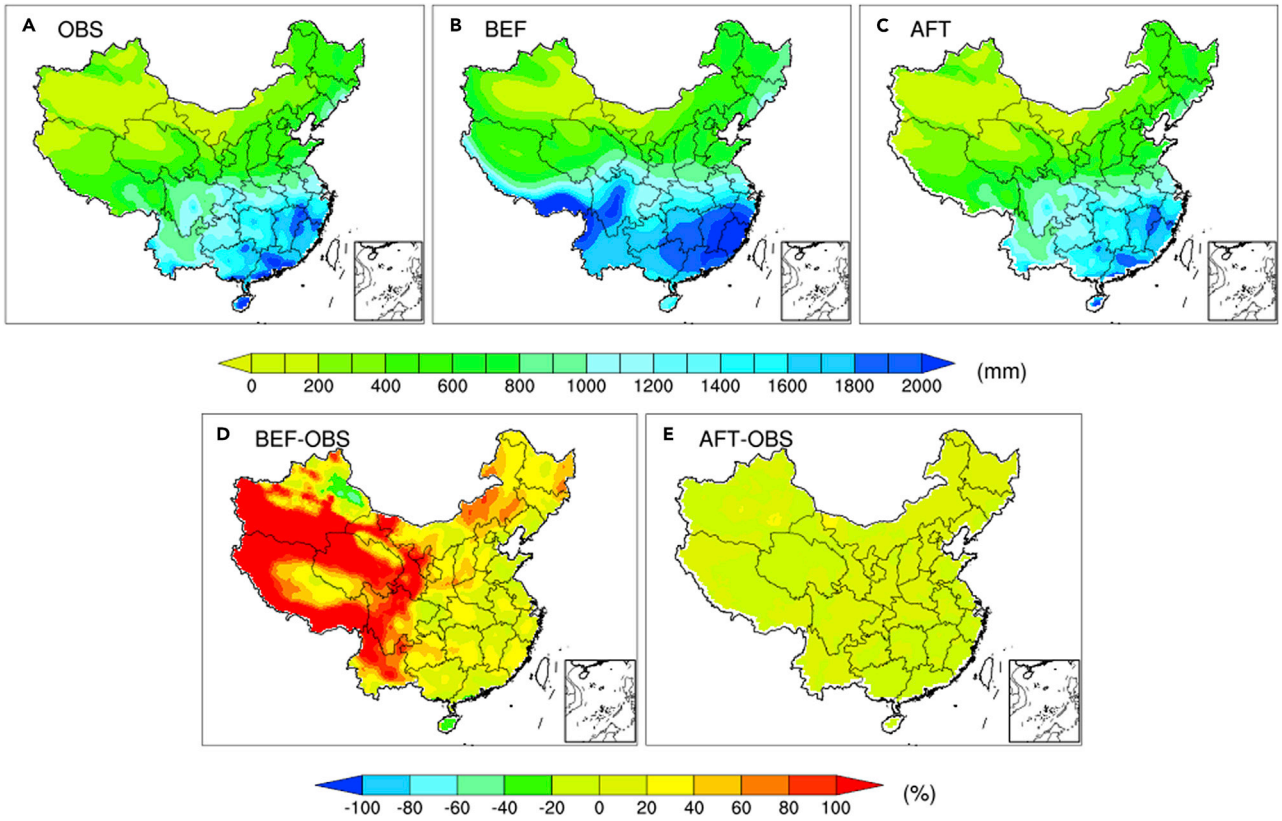

Figure 1. Comparison before and after bias correction for the multi-model ensemble mean (MME) in simulating the PRCPTOT for the baseline period (1995-2014)

(A) CN05.1 (OBS), (B) MME before bias correction (BEF), (C) MME after bias correction (AFT), (D) bias before correction (BEF-OBS), (E) bias after correction (AFT-OBS).

also are positive before correction but negative after correction in simulating the R99pTOT and R20mm. Compared with other indices, the improvement in simulating the CWD is not obvious based on the results of percentage biases. The whole CWD simulated by raw models and corrected ones is still overvalued in most parts of China, though the latter relative bias is smaller than the former. In view of spatial distribution, there are still biases over the west of China (i.e., Tibet Plateau) in simulating the R20mm and CWD.

Taylor diagram is used to evaluate quantitatively the performance of CMIP6 simulations in representing China's current climatological features of the above five extreme precipitation indices (Figure 3). It can be seen that, for each of these indices, the performance of models after correction is better than that before correction, especially for the PRCPTOT, Rx5day and R20mm. Take PRCPTOT for example, the correction coefficient is ~0.8 for the raw models and above 0.9 after bias correction for most models. Accordingly, the centered pattern root-mean-square difference is relatively low and the standard deviation is closer to the observation. The Taylor skill score (Figure S2) has also increased from ~0.5 to above 0.9. The score of bias correction is ranging from 0.6 to 0.8 for Rx5day, R20mm and CWD. The simulated skill of R99pTOT is the least among these indices from the Taylor diagram, with a correction coefficient of about 0.6 between simulations and observation. However, compared with the results before correction, the improvement is still obvious from the Taylor skill scores. In addition, the raw model ensemble in Taylor diagram is distributed loosely, suggesting the inter-model spread or uncertainty is larger in simulating these indices before correction. On contrary, there is inter-model consistency between the performances of the corrected CMIP6 members, especially for the PRCPTOT and R20mm, that is, the inter-model uncertainties of these indices are small when simulating the spatial pattern of precipitation extremes indices in China.

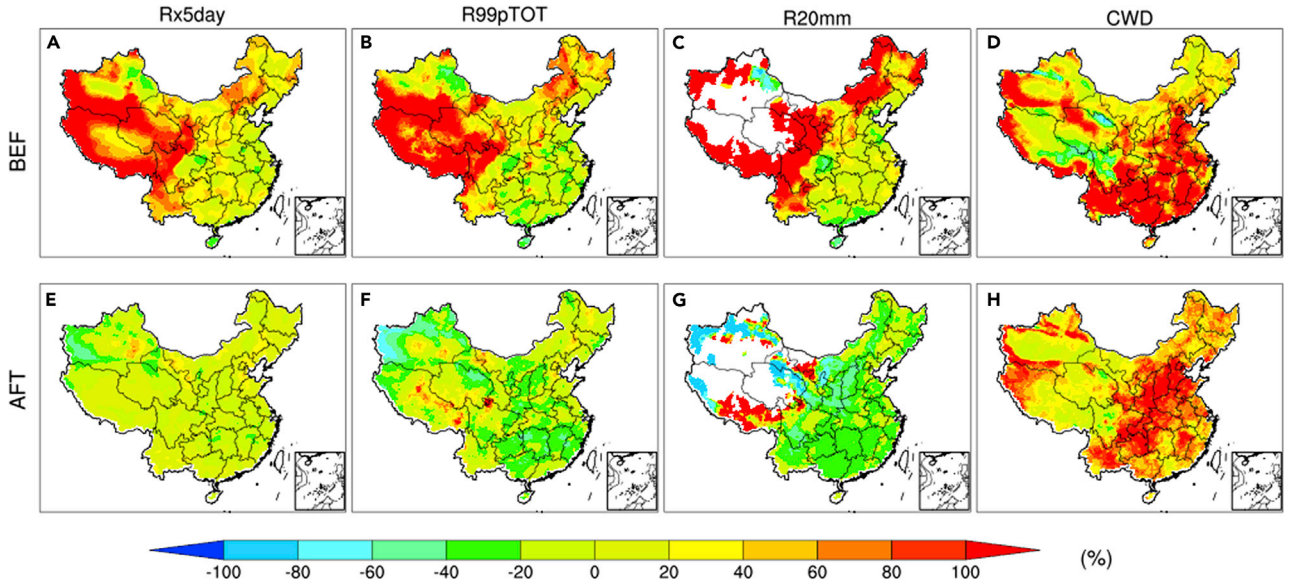

Figure 2. Spatial distribution of the difference between multi-model ensemble mean and observation for Rx5day
(A and E), R99pTOT (B and F), R20mm (C and G), CWD (D and H) in the baseline period (1995–2014). The first and second rows are the results of before and after correction, respectively.

Future changes

Probability distribution

Figure 4 shows the probability distribution of extreme precipitation events in the historical period and 1.5°C and 2.0°C global warming targets under SSP245, SSP370 and SSP585 scenarios over China. The overall distribution plots reveal that the curves for two warming periods tend to skew toward the right and have longer tails to some extent relative to the baseline period.

Over the whole of China, the distribution of the PRCPTOT in the 1.5°C and 2.0°C warming periods under the SSP scenarios suggests the annual total precipitation will increase as compared to the historical period. These curves are relatively normally distributed and the mean value increases from 600 mm in the historical period to above 650 mm in the future. In addition, with the increases in warming and emission scenario, future probability of occurring more annual total precipitation will become higher. A corresponding pattern distribution for the intensive extreme indices (i.e., Rx5day and R99pTOT) in two global warming levels under different emission scenarios has been observed. Like the PRCPTOT, there is also a distinguished shift in curves to the right side relative to the historical distribution. When the maximum consecutive 5-day precipitation is exceeding 80 mm and the annual strong precipitation amount is more than 120 mm, the probability of occurring heavy precipitation in the future is obviously larger than in the past. Especially for the R99pTOT, the curve becomes smoother and more flattened, indicating China is likely to occur more heavy precipitation events than in the baseline period. In terms of the R20mm, the curves produced under the high emission scenario are titled toward the right side. Compared with the future, the extreme heavy events exceeding 7 days in the baseline period are barely noticeable, which suggests the days of daily precipitation over 20 mm are likely to be more in future global warming scenarios. In the case of CWD, the results do not show a significant change in magnitude but slightly differ in the probability distribution between historical and future simulations, though there is still seen that the projected curves and their tails are more on the right and the maximum length of wet spell is likely up to 25 days.

Spatial distribution

In this section, the multi-model ensemble mean of projected changes in PRCPTOT, Rx5day, R99pTOT, R20mm and CWD for 1.5°C and 2.0°C warming levels under SSP245, SSP370 and SSP585 scenarios are analyzed.

The percentage and absolute changes in spatial distribution for the PRCPTOT under different scenarios are illustrated in Figure 5. Overall, though there is a slightly decreased precipitation in the northern region of

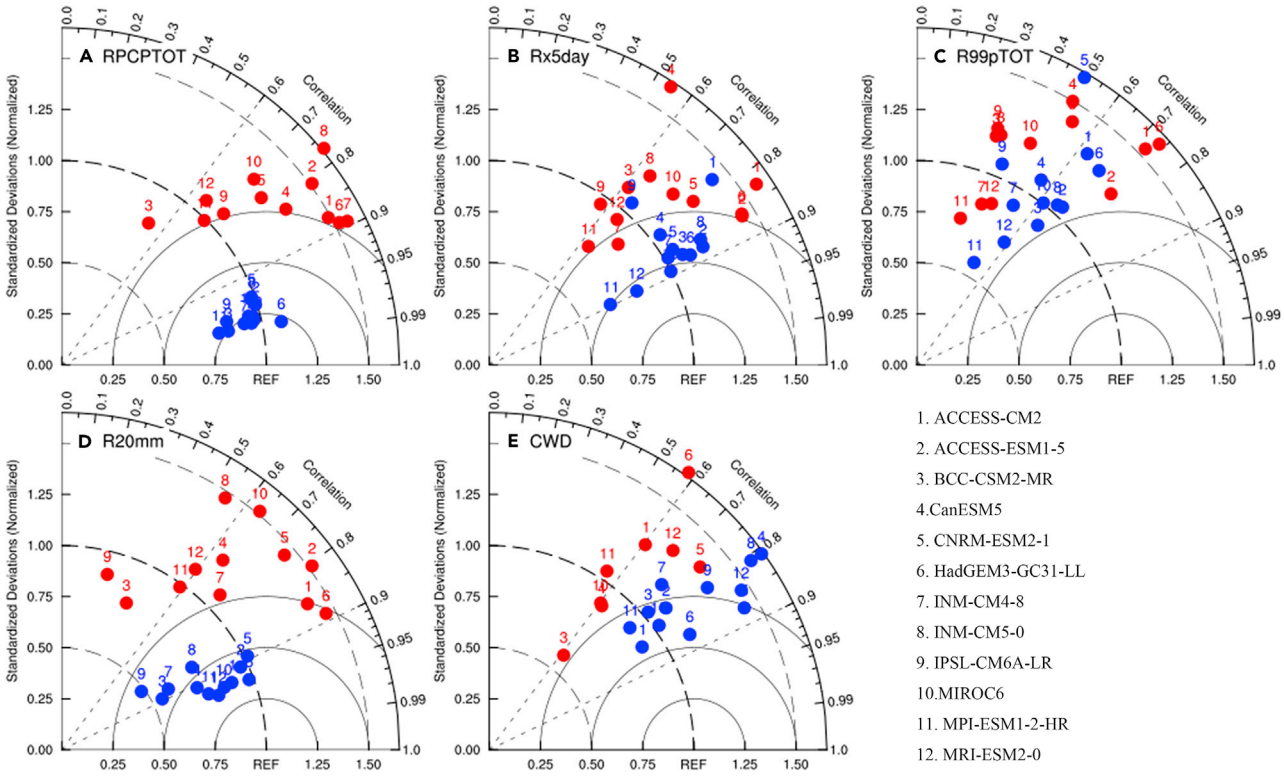

Figure 3. Taylor diagrams of 5 precipitation extreme indices between observation and CMIP6 models over China

Each dot represents a model identified by its number on the right bottom. The colors indicate the simulations before (red) and after (blue) correction respectively. The numbers represent the individual CMIP6 model.

Xinjiang, the annual total precipitation will increase by ~6%–10% overChina in the two warming levels (Table 1). Relative to the baseline period, the highest percentage increase magnitude for PRCPTOT is found in the south of Xinjiang and the west of Tibet, even exceeding 50%. However, the spatial distributions of absolute changes are different from the percentage results. The wet climatic zones (i.e., southeast of China) instead of the arid and semi-arid regions (i.e., the northwest) are inclined to receive more precipitation (~150 mm) at 1.5°C and 2.0°C warming levels. It is can be deciphered that the absolute changes are larger toward higher warming levels and emission scenarios compared with the reference period. In other words, under the 2.0°C global warming period and SSP585 emission scenario, the projected changes in some regions from the southeast to the north and along the Himalayas are more obvious.

The geographic structure of the anticipated changes in Rx5day, R99pTOT, R20mm and CWD across China relative to 1995–2014 are demonstrated in Figures 6 and S4. For Rx5day, the percentage changes in spatial grids are similar in most regions of China. The regional-averaged maximum consecutive 5-day precipitation will increase by 6.65%–9.95% from the SSP245–1.5 to SSP585–2.0 (Table 1). In spatial distribution, the south of Xinjiang and the west of Tibet have more increase than other regions. However, with regard to the reference period, the projected Rx5day is inclined to decrease by ~10% in the north of Xinjiang. Besides, it can be seen obviously that the changes in Rx5day show an increase in north and south areas over eastern China but a decrease in the middle in the 1.5°C global warming level and SSP245 scenario. This negative impact could be turned to positive when warming scenarios change from 1.5°C to 2.0°C, suggesting that likelihood of precipitation extremes in areas between the Yellow River and Yangtze River will increase with the temperature future warming. The R99pTOT represents the very heavy precipitation intensity. In total, the R99pTOT is projected to increase obviously across the whole of China. The intensification is found to be the utmost in the western region whereas the relatively low percentage increase is in the southeast despite a larger absolute increment in this region. The increasing magnitude of R99pTOT at two global warming levels is larger than other indices. With the accelerating global warming, the R99pTOT will have a minimum increase of ~23.65% (SSP245–1.5) and a maximum of 37.26% at different

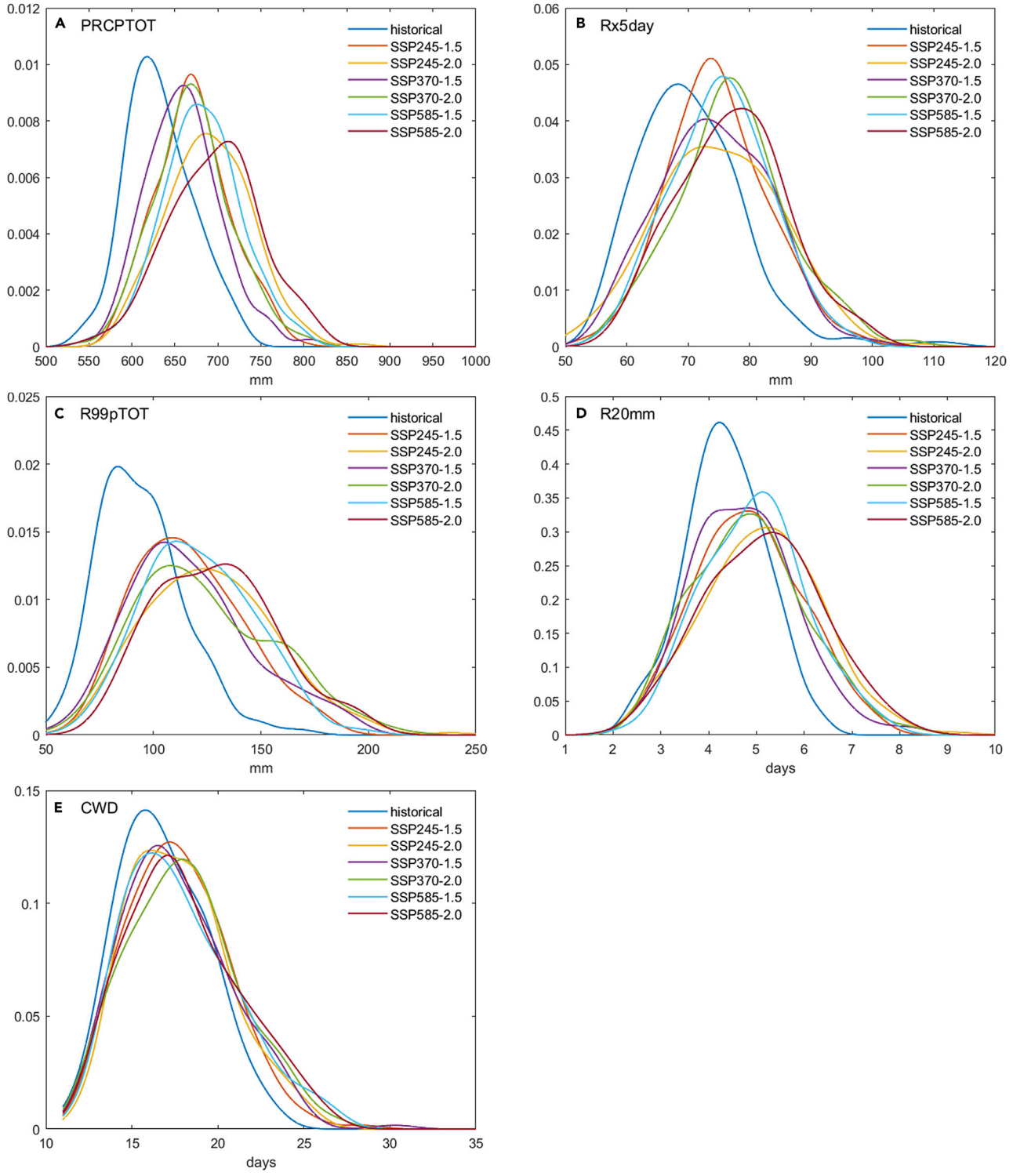

Figure 4. Probability distribution of changes in extreme precipitation indices in the historical and two global warming levels under SSP245, SSP370 and SSP585 scenarios

(A) PRCPTOT, (B) Rx5day, (C) R99pTOT, (D) R20mm, (E) CWD.

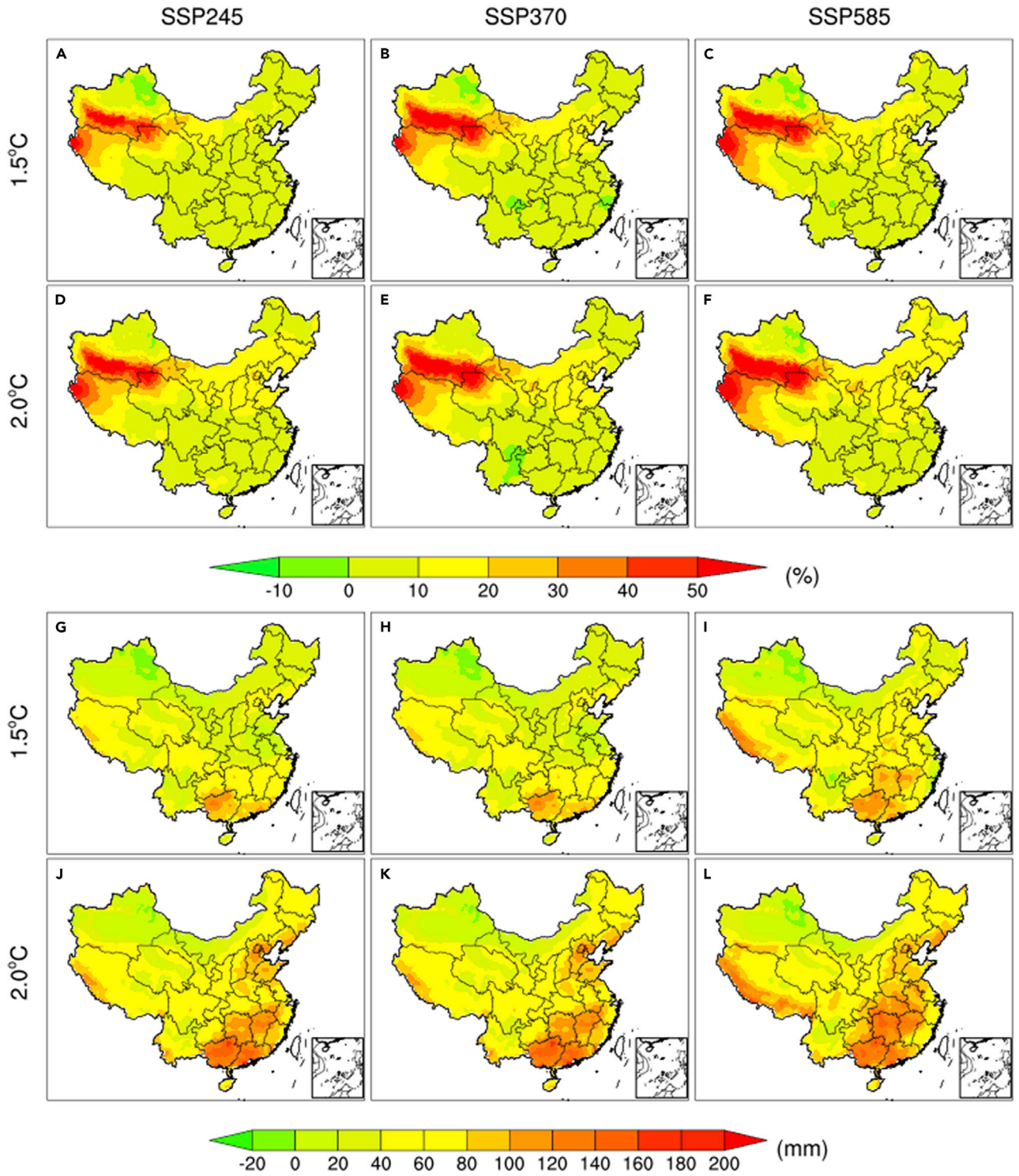

Figure 5. The changes in spatial distribution for PRCPTOT at 1.5°C and 2.0°C global warming targets under SSP245, SSP370 and SSP585 emission scenarios

The first and second rows are the percentage changes (A–F) and the second and fourth rows (G–L) indicate the absolute changes. The columns from left to right are under the SSP245, SSP370 and SSP585 scenarios, respectively.

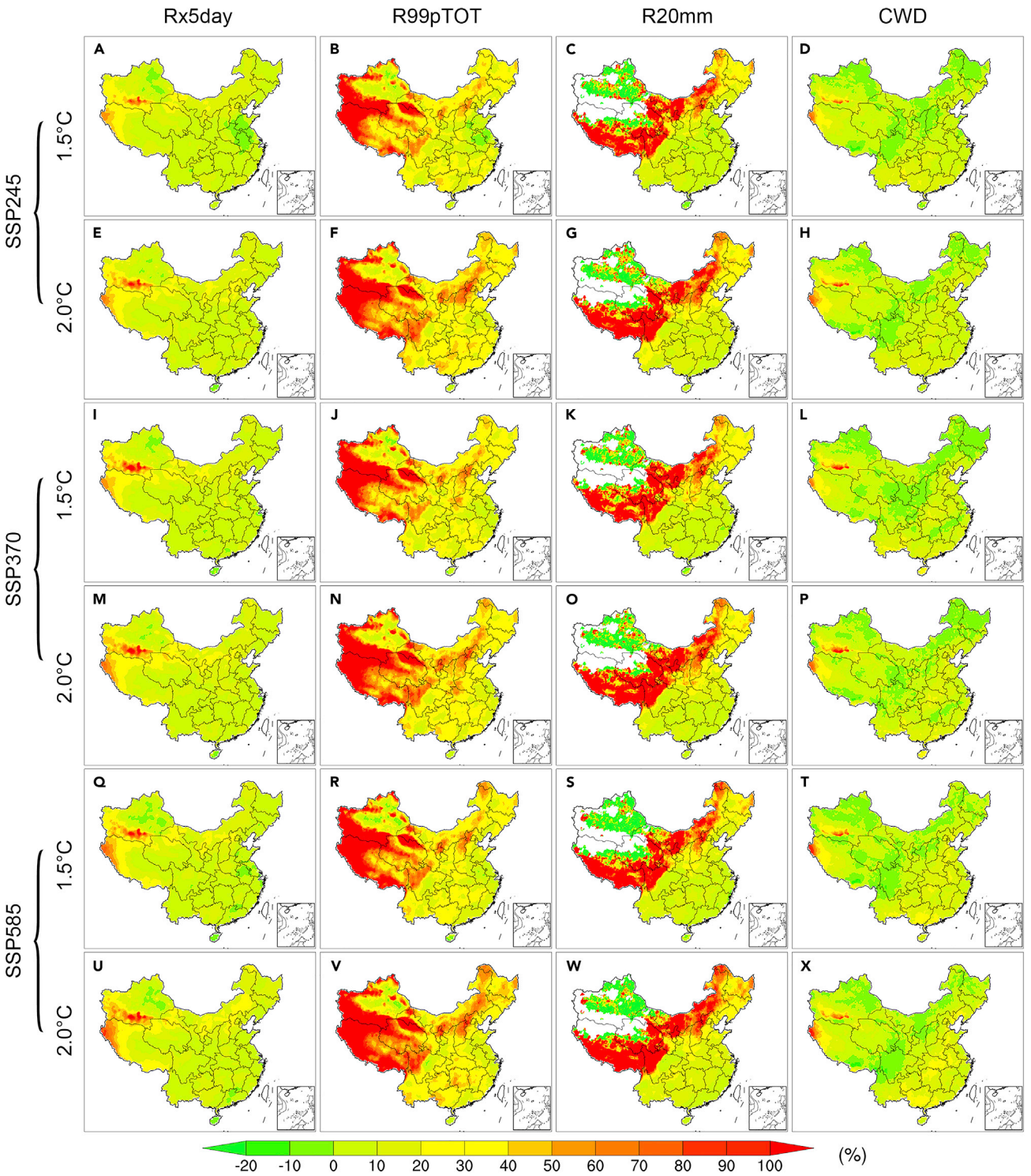

Figure 6. The percentage changes in spatial distribution for Rx5day (first column), R99pTOT (second column), R20mm (third column) and CWD (fourth column) at 1.5°C and 2.0°C global warming levels under SSP245

(A-H), SSP370 (I-P) and SSP585 (Q-X) emission scenarios.

Table 1. The area-averaged percentage changes for precipitation extreme indices overChina at 1.5°C and 2.0°C global warming targets under SSP245, SSP370 and SSP585 emission scenarios

	PRCPTOT	Rx5day	R99pTOT	R20mm	CWD
Baseline	623.83 mm	69.275 mm	93.152 mm	4.2457days	16.545days
SSP245–1.5	5.99%	6.65%	23.65%	11.20%	5.03%
SSP245–2.0	9.16%	9.81%	34.86%	18.13%	5.45%
SSP370–1.5	6.87%	6.77%	24.57%	11.20%	5.57%
SSP370–2.0	8.57%	8.85%	30.87%	14.69%	6.64%
SSP585–1.5	7.78%	7.83%	29.61%	13.62%	6.45%
SSP585–2.0	10.35%	9.95%	37.26%	18.68%	7.36%

warming scenarios for the whole domain. The projected changes in geographical characteristics of R20mm over China relative to the reference period (1995-2014) are similar basically to the R99pTOT. In response to global-scale warming, the frequency metric of precipitation extremes R20mm is intended to be the strongest over the south of Tibet Plateau and toward the northeastern Inner Mongolia of China under all the warming thresholds. For the entire domain, the R20mm is likely to be escalated by 11.20%–18.68% corresponding to the future warming world. However, the heavy precipitation days are exhibited to decrease (~10%) in most regions of Xinjiang. Regarding the distribution of CWD, the maximum length of wet spell is larger than that in the baseline period with an increase of ~5%–7%. The increasing magnitude is smaller relative to the other four indices. In spatial, the highest increase is mainly observed in the west of Tibet and parts of southern China, even exceeding 6 days. Likewise, the regional-averaged CWD is also projected to become higher with continued warming and emission levels. However, unlike other indices, the CWD is projected to have a slight decrease (~1 day) in some regions in China, such as the northeast, Inner Mongolia, Sichuan and the north of Xinjiang.

Moreover, despite different change magnitudes, almost all intensive and frequency precipitation extreme indices show an increasing trend under different warming thresholds with regard to the reference period from the view of the regional mean. There is one exception though, at the 2.0°C warming level the changes in these indices under the SSP370 seem to be smaller than those under the SSP245. Overall, the increasing magnitude of R99pTOT (~23%–37%) and R20mm (~11%–18%) is larger obviously than other indices. Thus, it is indicated that the increase in total precipitation is projected to be mainly because of a sharp increase in the intensity and days of very heavy precipitation in future global warming scenarios.

Avoided impacts of limiting global warming

IPCC 1.5°C special report indicated that the avoided climate change impacts on sustainable development, eradication of poverty and reducing inequalities would be greater if global warming were limited to 1.5°C rather than 2°C.[20] Thus, we will discuss how many percentages of increase of precipitation extremes would be reduced if global warming is locked at 1.5°C rather than the higher warming thresholds in this paper. The results in spatial distribution are illustrated in Figure 7.

There are differences in the percentage of changes in spatial distribution among indices. For the PRCPTOT, the higher increase magnitude (~50%) would be found in eastern China and Xinjiang in additional 0.5°C warming, whereas Tibet Plateau tends to have a relatively small increase. What's more, some regions, such as Qinghai and parts of southern China, have a decreasing trend for an additional 0.5°C warming. Two intensive extreme indices, such as Rx5day and R99pTOT, also are projected to have an increasing trend over most parts of China, especially in the southeastern region. In the case of R20mm and CWD, the changes in spatial distribution are indistinguishable on the fragmented map, that is, there is a mixture of increase and decrease for an additional 0.5°C.

However, the comparison is more clear in terms of the regional average for precipitation indices over China (Figure 8). The amplification in PRCPTOT is estimated to be increased by ~34% for an additional 0.5°C for the whole of China. Except for the west, the percentage change in annual total precipitation will decrease by above 30% if global-scale warming is limited to 1.5°C rather than higher warming threshold. When the global surface temperature increases further by 0.5°C, the projected largest impact of global warming would be on the southeast of China, where the precipitation extremes would increase by 39.6% (RX5day), 43.6% (R99pTOT) and

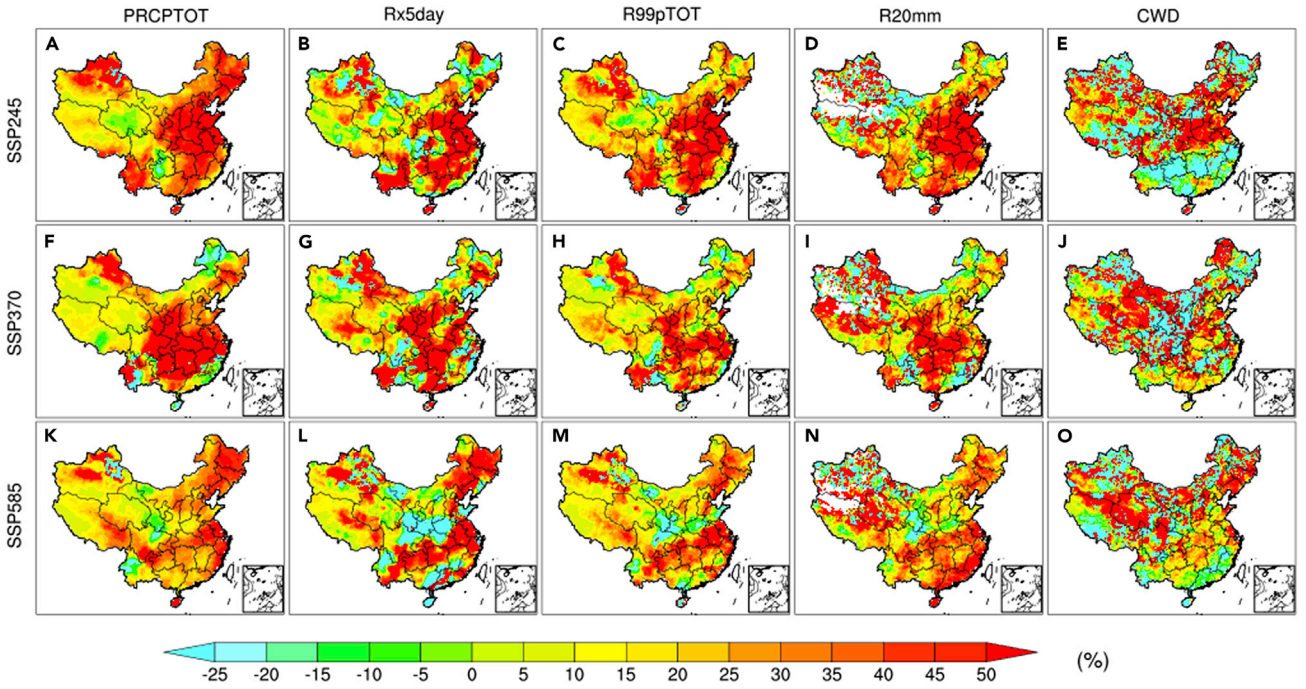

Figure 7. Spatial distribution of avoided impact in additional 0.5°C global warming for PRCPTOT (first column), Rx5day (second column), R99pTOT (third column), R20mm (fourth column) and CWD (fifth column) under SSP245
(A–E), SSP370 (F–J) and SSP585 (K–O) scenarios.

39.6% (R20mm). The increasing magnitude of precipitation intensity and frequency (except CWD) is greatly exceeding the global mean temperature changes (25%). In other words, if global-scale warming is limited to 1.5°C rather than higher warming threshold of 2.0°C, there will be an obvious benefit in the southeast of China. On the other hand, the west is likely to have less impact than other regions in adapting to the changes from 1.5°C to 2.0°C. In total, the PRCPTOT and R99pTOT are more sensitive to global warming whereas the maximum length of wet spell shows a smaller impact in an additional 0.5°C increase.

In addition, under the SSP585, the magnitude of avoided changes over China and its subregions seems to be smaller than those under the SSP245. The impact on the frequency of precipitation extremes (R20mm and CWD) in an additional 0.5°C for the west of China is larger under this higher emission scenario.

Moreover, similar to the analysis of the avoided impact on different global warming, we also depict the relative contribution to precipitation extremes from different emission pathways at the same warming level (Figure S5). According to Equation 4 in Methods section, we regard the SSP245 scenario as the baseline to calculate this relative contribution or avoided impact from the other two scenarios (i.e., SSP370 and SSP585). At the 1.5°C global warming level, relative to the SSP245 the overall contributions of total precipitation under SSP370 and SSP585 are positive (~20%) across most regions of China, particularly in the central-east areas, whereas the northwestern region shows a mixed distribution, in other words, both the positive and negative contributions are found in this region, suggesting the impact from different emission scenarios has more uncertainties. For two intensive indices, the spatial distributions of Rx5day and R99pTOT are consistent with the PRCPTOT. At the 1.5°C warming level, the central-east and northeastern local regions have the largest avoided impact. However, at the warming level of 2.0°C, because of a smaller Rx5day under SSP370, the relative contribution over southern China is smaller than that under SSP585. In addition, for two frequent indices, the avoided impact of CWD is larger than the R20mm, especially in the north of China.

The regional mean results can further compare the relative contributions from different emission scenarios on the changes in precipitation extremes (Figure S6). Obviously, the avoided impact from SSP585 is larger than SSP370, and the magnitude of contribution seems to be larger at the 1.5°C than that at the 2.0°C warming level. For example, the total precipitation will decrease above 20% from the SSP585 to SSP245

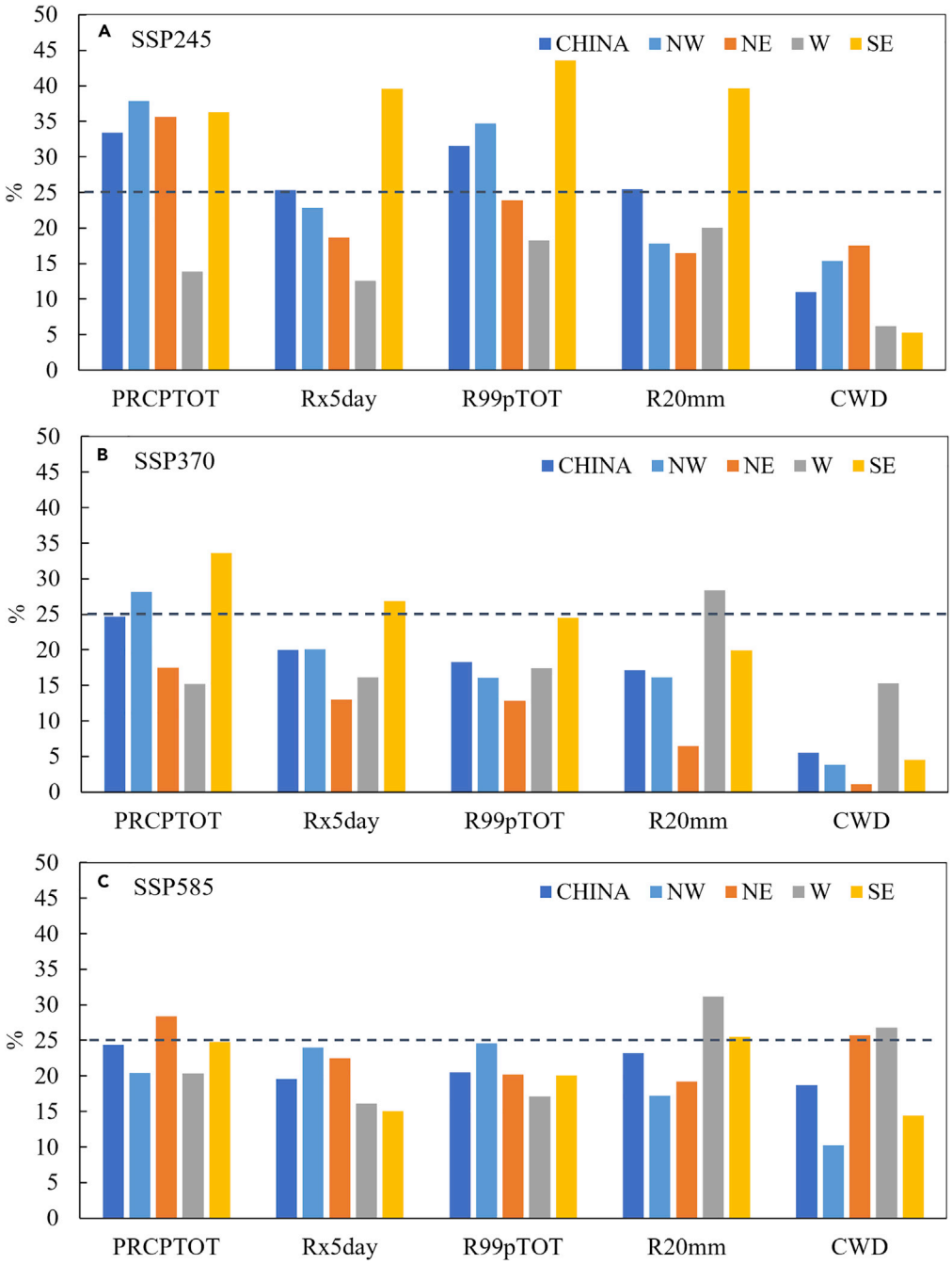

Figure 8. The area-averaged avoided impact of extreme precipitation indices from 0.5°C less warming over China and subregions under SSP245 (A), SSP370 (B) and SSP585 (C) scenarios

The 25% dashed line represents the percentage of change in global mean temperature from 2.0°C to 1.5°C.

at the 1.5°C warming level but ~10% at the 2.0°C level. Moreover, for the CWD, the contributions in the southeast and northeast are larger than those in the west and northwest of China. On the other hand, compared to the SSP245, the CWD has the largest impact relative to other indices under the SSP370. At the 1.5°C warming level, the overall contribution to the future changes in precipitation extremes is positive, with the largest impact magnitude in the northeast and northwest for PRCPTOT and CWD. On the other hand, at a 2.0°C warming level under SSP585, the R20mm in the northwest and CWD in the northeast tend to have larger contributions to the precipitation extremes in China. It is noted that except for the

CWD, the avoided impact for most indices shows a negative sign under the SSP370 and 2.0°C warming level because the precipitation extremes are projected to decrease slightly from SSP245 to SSP370.

DISCUSSIONS

Through bias correction, CMIP6 models show an obviously improving performance in reproducing patterns of the selected extreme precipitation indices in the baseline period, and the inter-model uncertainties in precipitation indices are also reduced. However, in view of spatial distribution, there are still biases over the west of China (i.e., Tibet Plateau) in simulating the R20mm and CWD. Overestimation in precipitation amount and frequency seems to be a common problem in climate models, particularly in Tibetan Plateau.[21] As the highest and most extensive highland in the world, these biases can be attributed because of the failure in detecting the summer monsoon signals,[22,23] unrealistic local vertical circulation and evaporation simulation,[24] and the indirect effects of sulfate aerosol[25] in climate models. On the other hand, the lack of reliable observed data because of the limited stations could be another possible reason.[26] Thus, considering the systematic model biases, we should be more prudent when using the forecasting simulating outputs to impact evaluation in this region. In addition to above reasons, the EDCDF bias correction method may also have some limitations when precipitation equals zeros for a given time series.[27] The precipitation in the arid northwest and alpine Tibet is very scarce, which could restrict the performance of EDCDF. Thus, an improvement of EDCDF bias method is needed in the future study.

Relative to the baseline period, our results show that China would experience more extreme precipitation events in both intensity and frequency under higher emissions and GWLs, although there are different magnitudes of changes in spatial distribution. For example, the highest percentage increase magnitude for PRCPTOT is found in the south of Xinjiang and the west of Tibet, even exceeding 50%, whereas the southeast is projected to receive more precipitation (~150 mm) based on the absolute results. The increasing magnitude of R99pTOT and R20mm is larger obviously than other indices, indicating that the increase in annual total precipitation is projected to be mainly because of a sharp increase in the intensity and days of very heavy precipitation in future global warming scenarios. Some studies came to a similar conclusion. Although the agreement in projected changes by different models is low in regions of complex topography, the projections from CMIP5, CMIP6 and CORDEX consistently show a percentage increase in heavy precipitation in higher latitude areas.[28,29] The reason for the larger percentage changes in the northwest is that the precipitation amounts in arid regions are inherently scarce, in other words, marginal changes in these regions will result in a large percentage variation and uniformity, implying it will increase the risk of precipitation extremes.[30] A previous study also reported similar findings over the southeast of China, that is, larger precipitation is projected to increase with higher emission levels in humid and semi-humid regions. In the subtropical and tropical humid regions of China, sunshine duration (i.e., shortwave radiation) is the primary cause of precipitation changes.[31]

Some previous studies have already demonstrated that heavy precipitation events overChina are likely to result from human-induced increases in greenhouse gases, especially under the SSP585 scenario.[30,32,33] The possible physical attributions behind the increase in frequency and intensity of extreme precipitation are various. One of the most dominant reasons is the increasing global temperature owing to anthropogenic influence. The warming increases the atmospheric water-holding capacity following the Clausius-Clapeyron (C-C) relation. This thermodynamic effect (moisture increase because of warming) leads to an increase in extreme precipitation at the global or local scales.[1] In addition, extreme precipitation can also be enhanced by dynamic responses and feedback that result from the atmospheric circulation change (i.e., ENSO, El Niños) to changes in the moisture flux convergence.[23,34] Liu et al. (2021)[35] investigated the link between Arctic amplification and extreme precipitation in the Northern Hemisphere, they found the Arctic amplification will continue to enhance with the increase in global temperature in the future, resulting in more persistent weather patterns and more extreme weather events, particularly under the SSP585 scenario. Moreover, at the local and regional scales, the regional feedbacks forcings (i.e., land use or aerosol concentrations changes) also affect the frequency and intensity of precipitation extremes.[24,36]

In addition, an additional 0.5°C warming can lead to a further increase in precipitation extremes over China. Except for the west, the avoided impact on annual total precipitation will be above 30% under SSP245. If global-scale warming is limited to 1.5°C rather than higher warming threshold, the projected largest impact of global warming would be on the southeast of China. Moreover, the avoided impact of increasing 0.5°C for precipitation extremes is larger under the SSP245 scenario. In summary, we conclude that limiting

global warming to 1.5°C instead of 2°C would have substantial benefits for China in terms of reducing occurrences of extreme precipitation events. That is in agreement with other studies, showing that every bit of global warming matters and that changes in global warming of 0.5°C lead to statistically significant changes in mean climate and climate extremes on a global scale and for large regions.[1]

Limitations of the study

This study also has strong implications for implementing global emissions mitigation goals designed under the Paris Agreement of 2015. However, it should be noted that in this study the global warming levels extracted from the SSP-RCP scenarios, i.e., 1.5°C and 2°C, are not representative of the aims of the Paris Agreement. Because it's generally understood that the Paris Agreement implicitly refers to quasi-stabilized climate states[37] and that there is a difference in climate between rapid warming and stabilized climate states.[38,39] In addition, the timing of reaching global warming levels between CMIP6 models is different, and it may also be related to internal climate variability[40,41] and aerosol effects[42] in models. On the other hand, it should be mentioned that there are some unavoidable uncertainties in the projection of future extreme precipitation change. These uncertainties can arise from climate models, climate scenarios, bias correction, etc.[31] Thus, it is suggested that more models and emission scenarios under the CMIP6 family should be included when conducting climate projections in the future study.

Conclusion

In this paper, we have investigated the future changes in extreme events associated with daily precipitation under 1.5°C and 2.0°C global warming thresholds across China using a bias-corrected CMIP6 ensemble using an EDCDF method. The impact of an additional 0.5°C (2.0–1.5°C) of warming and the relative contribution of different emission pathways on precipitation-related indices over China are further analyzed.

Overall, compared with the observation CN05.1, bias-corrected CMIP6 models have an apparent improvement in reproducing patterns of the selected extreme precipitation indices in the baseline period (1995–2014) in terms of spatial distribution and Taylor diagram. In spatial, except for CWD, the biases in the east of China are smaller than in the west and the overvalued biases in the west are corrected thoroughly through bias correction. The results from the Taylor diagram show that PRCPTOT, Rx5day and R20mm simulation competence are better than that of R99pTOT and CWD in China. Through bias correction, the inter-model uncertainties in precipitation indices are also reduced. However, in view of spatial distribution, there are still biases over the west of China (i.e., Tibet Plateau) in simulating the R20mm and CWD.

Future responses of precipitation extremes overChina at 1.5°C and 2.0°C global warming levels under SSP245, SSP370 and SSP585 scenarios are further investigated. Overall, China would experience more extreme precipitation events in both intensity and frequency under higher emissions and GWLs, in terms of probability distributions and spatial changes in five precipitation indices. The annual total precipitation for the regional average tends to increase by ~6% at least under SSP245–1.5 and ~10% at most under SSP585–2.0 scenario. The highest percentage increase magnitude for PRCPTOT is found in the south of Xinjiang and the west of Tibet, whereas the southeast is projected to receive more precipitation based on the absolute results. The increasing magnitude of R99pTOT and R20mm is larger obviously than other indices, indicating that the increase in annual total precipitation is projected to be mainly because of a sharp increase in the intensity and days of very heavy precipitation in future global warming scenarios.

Moreover, our results show that an additional 0.5°C warming can lead to a further increase in precipitation extremes over China, and the projected largest impact of global warming would be on the southeast of China. We also analyzed the relative contribution of different emission pathways to the changes in precipitation extremes. The results show that at the same warming level the avoided impact from SSP585 is larger than SSP370, especially at a 2.0 warming level for R20mm in the northwest and CWD in the northeast of China. Meanwhile, the magnitude of contribution seems to be larger at the 1.5°C than that at the 2.0°C warming level. Under the SSP370 scenario, the CWD has the largest impact relative to other indices. In summary, we conclude that limiting global warming to 1.5°C and low emission pathways (i.e., SSP245) instead of 2°C and high emission pathways (i.e., SSP585) would have substantial benefits for China in terms of reducing occurrences of extreme precipitation events.

STAR★METHODS

Detailed methods are provided in the online version of this paper and include the following:

- KEY RESOURCES TABLE
- RESOURCE AVAILABILITY
  - Lead contact
  - Materials availability
  - Data and code availability
- METHOD DETAILS
  - Bias correction to the CMIP6 data
  - Timing of two warming levels
  - Validation method and observation
  - Extreme precipitation indices
  - Quantification of the avoided impacts

SUPPLEMENTAL INFORMATION

Supplemental information can be found online at https://doi.org/10.1016/j.isci.2023.106179.

ACKNOWLEDGMENTS

This paper is supported by the National Key Research and Development Program of China (Grant No. 2018YFE0208400), the Science and Technology Project of State Grid Corporation of China (Key Technologies of Novel Integrated Energy System Considering Cross-border Interconnection).

AUTHOR CONTRIBUTIONS

J.G. and Y.S. conceptualized this research. X.W. designed the research methods. L.L. processed and analyzed the data. Z.L. wrote the paper. X.W. and X.L. made revisions to the paper. All the authors conceived the paper and designed the research.

DECLARATION OF INTERESTS

The authors declare no competing interests.

Received: July 14, 2022
Revised: November 24, 2022
Accepted: February 7, 2023
Published: February 14, 2023

REFERENCES

1. Allan, R.P., Hawkins, E., Bellouin, N., and Collins, B. (2021). IPCC, 2021: Summary for Policymakers.

2. Mondal, S.K., Huang, J., Wang, Y., Su, B., Kundzewicz, Z.W., Jiang, S., Zhai, J., Chen, Z., Jing, C., and Jiang, T. (2022). Changes in extreme precipitation across South Asia for each 0.5 C of warming from 1.5 C to 3.0 C above pre-industrial levels. Atmos. Res. *266*, 105961.

3. Li, H., Li, Z., Chen, Y., Xiang, Y., Liu, Y., Kayumba, P.M., and Li, X. (2021). Drylands face potential threat of robust drought in the CMIP6 SSPs scenarios. Environ. Res. Lett. *16*, 114004.

4. Liu, W., Sun, F., Lim, W.H., Zhang, J., Wang, H., Shiogama, H., and Zhang, Y. (2018). Global drought and severe drought-affected populations in 1.5 and 2 C warmer worlds. Earth Syst. Dyn. *9*, 267–283.

5. CRED (2022). 2021 Disasters in Numbers.

6. UNFCC (2015). FCCC/CP/2015/L.9/Rev.1: Adoption of the Paris Agreement (UNFCCC), pp. 1–32.

7. Nangombe, S., Zhou, T., Zhang, W., Wu, B., Hu, S., Zou, L., and Li, D. (2018). Record-breaking climate extremes in Africa under stabilized 1.5 C and 2 C global warming scenarios. Nat. Clim. Chang. *8*, 375–380.

8. Paltán, H.A., Pant, R., Plummer Braeckman, J., and Dadson, S.J. (2021). Increased water risks to global hydropower in 1.5° C and 2.0° C Warmer Worlds. J. Hydrol. *599*, 126503.

9. Sieck, K., Nam, C., Bouwer, L.M., Rechid, D., and Jacob, D. (2021). Weather extremes over Europe under 1.5 and 2.0° C global warming from HAPPI regional climate ensemble simulations. Earth Syst. Dyn. *12*, 457–468.

10. Chen, S., and Yuan, X. (2021). CMIP6 projects less frequent seasonal soil moisture droughts over China in response to different warming levels. Environ. Res. Lett. *16*, 044053.

11. Jiang, Z., Hou, Q., Li, T., Liang, Y., and Li, L. (2021). Divergent responses of summer precipitation in China to 1.5 C global warming in transient and stabilized scenarios. Earth's Future *9*. e2020EF001832.

12. Ayugi, B., Dike, V., Ngoma, H., Babaousmail, H., Mumo, R., and Ongoma, V. (2021). Future changes in precipitation extremes over East Africa based on CMIP6 models. Water *13*, 2358.

13. Zhu, H., Jiang, Z., and Li, L. (2021). Projection of climate extremes in China, an incremental exercise from CMIP5 to CMIP6. Sci. Bull. *66*, 2528–2537.

14. Lim Kam Sian, K.T.C., Hagan, D.F.T., Ayugi, B.O., Nooni, I.K., Ullah, W., Babaousmail, H., and Ongoma, V. (2022). Projections of precipitation extremes based on bias-corrected CMIP6 models ensemble over

Southern Africa. Int. J. Climatol. *42*, 8269–8289.

15. Babaousmail, H., Hou, R., Ayugi, B., Sian, K.T.C.L.K., Ojara, M., Mumo, R., Chehbouni, A., and Ongoma, V. (2022). Future changes in mean and extreme precipitation over the Mediterranean and Sahara regions using bias-corrected CMIP6 models. Int. J. Climatol. *42*, 7280–7297.

16. Yang, L., Tian, J., Fu, Y., Zhu, B., He, X., Gao, M., Odamtten, M.T., Kong, R., and Zhang, Z. (2022). Will the arid and semi-arid regions of Northwest China become warmer and wetter based on CMIP6 models? Nord. Hydrol *53*, 29–50.

17. Chen, L., and Frauenfeld, O.W. (2014). A comprehensive evaluation of precipitation simulations over China based on CMIP5 multimodel ensemble projections. J. Geophys. Res. Atmos. *119*, 5767–5786.

18. Tokarska, K.B., Stolpe, M.B., Sippel, S., Fischer, E.M., Smith, C.J., Lehner, F., and Knutti, R. (2020). Past warming trend constrains future warming in CMIP6 models. Sci. Adv. *6*, eaaz9549.

19. Mishra, V., Bhatia, U., and Tiwari, A.D. (2020). Bias-corrected climate projections for South Asia from coupled model intercomparison project-6. Sci. Data *7*, 338.

20. Masson-Delmotte, V., Zhai, P., Portner, H., Roberts, D., Skea, J., Shukla, P., Pirani, A., Moufouma-Okia, W., Péan, C., and Pidcock, R. (2018). Global warming of 1.5 [degrees] C. An IPCC special report on the impacts of global warming of 1.5 [degrees] C above pre-industrial levels and related global greenhouse gas emission pathways. In the Context of Strengthening the Global Response to the Threat of Climate Change. Sustainable Development, and Efforts to Eradicate Poverty.

21. Liang-Liang, L., Jian, L., and Ru-Cong, Y. (2022). Evaluation of CMIP6 HighResMIP models in simulating precipitation over central Asia. Adv. Clim. Change Res. *13*, 1–13.

22. Mizuta, R., and Endo, H. (2020). Projected changes in extreme precipitation in a 60-km AGCM large ensemble and their dependence on return periods. Geophys. Res. Lett. *47*. e2019GL086855.

23. Lee, D., Min, S.-K., Jin, J., Lee, J.-W., Cha, D.-H., Suh, M.-S., Ahn, J.-B., Hong, S.-Y., Kang, H.-S., and Joh, M. (2017). Thermodynamic and dynamic contributions to future changes in summer precipitation over Northeast Asia and Korea: a multi-RCM study. Clim. Dyn. *49*, 4121–4139.

24. Hirsch, A.L., Guillod, B.P., Seneviratne, S.I., Beyerle, U., Boysen, L.R., Brovkin, V., Davin, E.L., Doelman, J.C., Kim, H., Mitchell, D.M., et al. (2018). Biogeophysical impacts of land-use change on climate extremes in low-emission scenarios: results from HAPPI-Land. Earth's Future *6*, 396–409.

25. Duan, A., Hu, J., and Xiao, Z. (2013). The Tibetan Plateau summer monsoon in the CMIP5 simulations. J. Clim. *26*, 7747–7766.

26. Bucchignani, E., Montesarchio, M., Cattaneo, L., Manzi, M.P., and Mercogliano, P. (2014). Regional climate modeling over China with COSMO-CLM: performance assessment and climate projections. J. Geophys. Res. Atmos. *119*, 12,151–12,170.

27. Wang, L., and Chen, W. (2014). Equiratio cumulative distribution function matching as an improvement to the equidistant approach in bias correction of precipitation. Atmos. Sci. Lett. *15*, 1–6.

28. Wester, P., Mishra, A., Mukherji, A., and Shrestha, A.B. (2019). The Hindu Kush Himalaya Assessment: Mountains, Climate Change, Sustainability and People (Springer Nature).

29. Coppola, E., Nogherotto, R., Ciarlo', J.M., Giorgi, F., Meijgaard, E., Kadygrov, N., Iles, C., Corre, L., Sandstad, M., Somot, S., et al. (2021). Assessment of the European climate projections as simulated by the large EURO-CORDEX regional and global climate model ensemble. JGR. Atmospheres *126*. e2019JD032356.

30. Duan, W., Zou, S., Christidis, N., Schaller, N., Chen, Y., Sahu, N., Li, Z., Fang, G., and Zhou, B. (2022). Changes in temporal inequality of precipitation extremes over China due to anthropogenic forcings. npj Clim. Atmos. Sci. *5*, 33.

31. Su, B., Huang, J., Mondal, S.K., Zhai, J., Wang, Y., Wen, S., Gao, M., Lv, Y., Jiang, S., Jiang, T., and Li, A. (2021). Insight from CMIP6 SSP-RCP scenarios for future drought characteristics in China. Atmos. Res. *250*, 105375.

32. Xu, K., Xu, B., Ju, J., Wu, C., Dai, H., and Hu, B.X. (2019). Projection and uncertainty of precipitation extremes in the CMIP5 multimodel ensembles over nine major basins in China. Atmos. Res. *226*, 122–137.

33. Chen, H., Sun, J., Lin, W., and Xu, H. (2020). Comparison of CMIP6 and CMIP5 models in simulating climate extremes. Sci. Bull. *65*, 1415–1418.

34. Freychet, N., Hsu, H.-H., Chou, C., and Wu, C.-H. (2015). Asian summer monsoon in CMIP5 projections: a link between the change in extreme precipitation and monsoon dynamics. J. Clim. *28*, 1477–1493.

35. Liu, J., Wu, D., Xu, X., Ji, M., Chen, Q., and Wang, X. (2021). Projection of extreme precipitation induced by Arctic amplification over the Northern Hemisphere. Environ. Res. Lett. *16*, 074012.

36. Findell, K.L., Berg, A., Gentine, P., Krasting, J.P., Lintner, B.R., Malyshev, S., Santanello, J.A., and Shevliakova, E. (2017). The impact of anthropogenic land use and land cover change on regional climate extremes. Nat. Commun. *8*, 989.

37. Rogelj, J., Schleussner, C.F., and Hare, W. (2017). Getting it right matters: temperature goal interpretations in geoscience research. Geophys. Res. Lett. *44*, 10662–10665.

38. King, A.D., Lane, T.P., Henley, B.J., and Brown, J.R. (2020). Global and regional impacts differ between transient and equilibrium warmer worlds. Nat. Clim. Chang. *10*, 42–47.

39. Rugenstein, M., Bloch-Johnson, J., Abe-Ouchi, A., Andrews, T., Beyerle, U., Cao, L., Chadha, T., Danabasoglu, G., Dufresne, J.-L., Duan, L., et al. (2019). LongRunMIP: motivation and design for a large collection of millennial-length AOGCM simulations. Bull. Am. Meteorol. Soc. *100*, 2551–2570.

40. Henley, B.J., and King, A.D. (2017). Trajectories toward the 1.5 C Paris target: modulation by the interdecadal Pacific oscillation. Geophys. Res. Lett. *44*, 4256–4262.

41. Smith, D.M., Scaife, A.A., Hawkins, E., Bilbao, R., Boer, G.J., Caian, M., Caron, L.P., Danabasoglu, G., Delworth, T., Doblas-Reyes, F.J., et al. (2018). Predicted chance that global warming will temporarily exceed 1.5 C. Geophys. Res. Lett. *45*, 11895–11903.

42. Dittus, A.J., Hawkins, E., Wilcox, L.J., Sutton, R.T., Smith, C.J., Andrews, M.B., and Forster, P.M. (2020). Sensitivity of historical climate simulations to uncertain aerosol forcing. Geophys. Res. Lett. *47*. e2019GL085806.

43. Xu, H., Chen, H., and Wang, H. (2022). Future changes in precipitation extremes across China based on CMIP6 models. Int. J. Climatol. *42*, 635–651.

44. Yang, X., Zhou, B., Xu, Y., and Han, Z. (2021). CMIP6 evaluation and projection of temperature and precipitation over China. Adv. Atmos. Sci. *38*, 817–830.

45. Song, Z., Xia, J., She, D., Li, L., Hu, C., and Hong, S. (2021). Assessment of meteorological drought change in the 21st century based on CMIP6 multi-model ensemble projections over mainland China. J. Hydrol. *601*, 126643.

46. O'Neill, B.C., Tebaldi, C., Van Vuuren, D.P., Eyring, V., Friedlingstein, P., Hurtt, G., Knutti, R., Kriegler, E., Lamarque, J.-F., Lowe, J., et al. (2016). The scenario model intercomparison project (ScenarioMIP) for CMIP6. Geosci. Model Dev. *9*, 3461–3482.

47. Wei, L., Liu, L., Jing, C., Wu, Y., Xin, X., Yang, B., Tang, H., Li, Y., Wang, Y., Zhang, T., and Zhang, F. (2022). Simulation and projection of climate extremes in China by a set of statistical downscaled data. Int. J. Environ. Res. Public Health *19*, 6398.

48. Tian, J., Zhang, Z., Ahmed, Z., Zhang, L., Su, B., Tao, H., and Jiang, T. (2021). Projections of precipitation over China based on CMIP6 models. Stoch. Environ. Res. Risk Assess. *35*, 831–848.

49. Zhao, Y., Qian, C., Zhang, W., He, D., and Qi, Y. (2021). Extreme temperature indices in

Eurasia in a CMIP6 multi-model ensemble: evaluation and projection. Int. J. Climatol. *41*, 5368–5385.

50. Taylor, K.E. (2001). Summarizing multiple aspects of model performance in a single diagram. J. Geophys. Res. *106*, 7183–7192.

51. Guo, J., Huang, G., Wang, X., Li, Y., and Yang, L. (2018). Future changes in precipitation extremes over China projected by a regional climate model ensemble. Atmos. Environ. *188*, 142–156.

52. Wu, J., and GAO, X.-J. (2013). A gridded daily observation dataset over China region and comparison with the other datasets. Chin. J. Geophys. *56*, 1102–1111.

53. Zhou, B., Xu, Y., Wu, J., Dong, S., and Shi, Y. (2016). Changes in temperature and precipitation extreme indices over China: analysis of a high-resolution grid dataset. Int. J. Climatol. *36*, 1051–1066.

54. Nie, Y., and Sun, J. (2020). Evaluation of high-resolution precipitation products over southwest China. J. Hydrometeorol. *21*, 2691–2712.

55. Zhu, Y.-Y., and Yang, S. (2020). Evaluation of CMIP6 for historical temperature and precipitation over the Tibetan Plateau and its comparison with CMIP5. Adv. Clim. Change Res. *11*, 239–251.

56. Sillmann, J., Kharin, V.V., Zhang, X., Zwiers, F.W., and Bronaugh, D. (2013). Climate extremes indices in the CMIP5 multimodel ensemble: Part 1. Model evaluation in the present climate. J. Geophys. Res. Atmos. *118*, 1716–1733.

57. Li, D., Qi, Y., and Zhou, T. (2021). Changes in rainfall erosivity over mainland China under stabilized 1.5°C and 2°C warming futures. J. Hydrol. *603*, 126996.

STAR★METHODS

KEY RESOURCES TABLE

REAGENT or RESOURCE	SOURCE	IDENTIFIER
Deposited data		
CN05.1 dataset	China Meteorological Administration	http://www.nmic.cn/
CMIP6 dataset	World Climate Research Program (WCRP)	https://esgf-node.llnl.gov/search/cmip6/

RESOURCE AVAILABILITY

Lead contact

Further information and requests for data and code files should be directed to and will be fulfilled by the lead contact, Yangshuo Shen (shenyangshuo@163.com).

Materials availability

This study did not generate new unique reagents.

Data and code availability

Any additional information required to reanalyze the data reported in this paper is available from the lead contact upon request.

METHOD DETAILS

Bias correction to the CMIP6 data

Precipitation from the GCM has a bias due to their coarse resolution or model parameterizations. Thus, downscaling and bias correction is required for the assessment of extreme precipitation changes and impacts. Here, we referred to previous literature about the performance assessment of CMIP6 in simulating the present or historical climatology for different regions worldwide, particularly in China.[43–45] Based on this, the daily precipitation output from 12 raw climate models of CMIP6 in the historical period of 1995-2014, and in the future period of 2015-2100 under SSP2-RCP4.5 (SSP245), SSP3-RCP7.0 (SSP370) and SSP5-RCP8.5 (SSP585) emission scenarios, are selected for further downscaling and bias correction in this study (see Table S1). SSP245 represents an intermediate scenario, in which current tendencies in climate change remain constant. SSP370 is the medium to the high end of the range of future forcing pathways. SSP585 is a scenario in which no policies regarding the emission of GHGs are applied, leading to intensive fossil-fuel consumption.[46] These scenarios represent future forcing pathways of 4.5 Wm^{-2}, 7.0 Wm^{-2} and 8.5 Wm^{-2} in 2100, respectively.

The raw daily CMIP6 simulations are bias-corrected with an equidistant cumulative distribution functions (EDCDF) method. The EDCDF is based on the quantile mapping technology, which assumes that the difference between the observation and the simulation in the training period is the same in any selected simulation period for a given percentile.[47,48] The daily precipitation used in this study is fitted based on the mixed gamma distribution. Then, original GCM datasets are bias-corrected by adding the difference to agree with that of observations in a given reference period. This approach is defined as follows:

$$\tilde{x}_{m-p} = x_{m-p} + F^{-1}_{o-c}\left(F_{m-p}\left(x_{m-p}\right)\right) - F^{-1}_{m-c}\left(F_{m-p}\left(x_{m-p}\right)\right) \quad \text{(Equation 1)}$$

where $\tilde{x}_{m-p}$ is corrected daily precipitation from CMIP6 in future period; x_{m-p} is the projected original precipitation; F_{m-p} refers to the cumulative distribution function of the model for future projection period; F^{-1}_{o-c} and F^{-1}_{m-c} are the quantile functions for observation and models in the reference period, respectively.

Timing of two warming levels

In this paper, a time sampling approach is used to calculate different warming levels.[2,11,49] For each GCM model output, a 20-year moving mean of the global annual mean surface temperature is firstly computed. We calculated the first year reaching the specific warming level (i.e., 1.5°C and 2.0°C) above the preindustrial period (1850-1900) for each model. For the ensemble mean, we obtained 2028 (2026) and 2046 (2039)

as the year of reaching 1.5°C and 2.0°C global warming targets under the SSP245 (SSP585) scenario (Figure S3). Then, a 20-year window extending from 10 years prior and 9 years after the timing is attained at the 1.5°C and 2.0°C global warming levels for each CMIP6 model (Table S2). All the intended extreme precipitation indices statistics are calculated individually in the 20-year target window, afterwards, the mean value of the multi-model ensemble with all the certain SSP scenarios are obtained for individual warming threshold. In addition, the same length window (1995-2014) is as the baseline or historical period to validate the performance of CMIP6.

Validation method and observation

The Taylor diagram[50] is employed to test the skill of the bias-corrected CMIP6 data in simulating the spatial pattern of extreme precipitation indices during the baseline period. From the Taylor diagram, three estimated indicators, such as the spatial correlation coefficient (R), the centered pattern root-mean-square difference (CRMSD) and the ratio of standard deviations (RSD) between CMIP6 ensemble and observation, can be presented intuitively and compared easily among models. In the diagram, angular axes show the spatial correlation coefficient between simulations and observation, which quantifies the degree of phase agreement of two datasets. Radial axes centered on the coordinate origin and 'REF' point (representing the observation) show the normalized spatial standard deviations and centered pattern root-mean square difference, respectively. If the spatial correlation and ratio of standard deviations are close to 1 and the centered pattern root-mean-square difference is close to the 'REF' point, it means the performance of model is better.[49,51] In addition, to evaluate comprehensively above three performance skills from Taylor diagram, a skill score is used:

$$S = \frac{4(1+R)^4}{(RSD+1/RSD)^2(1+R_0)^4} \quad \text{(Equation 2)}$$

where S is the Taylor skill score, R is the pattern correlation between the models and the observation, RSD is the ratio of spatial standard deviation in the models against that of the observation. R_0 is the maximum correlation coefficient attainable (here we use 0.999). The score equals 1 for a perfect match between the model and observation, and 0 for an inverse model performance.[13,50]

In this study, the observed daily precipitation for validation is from the CN05.1 dataset, which is developed by the National Climate Center, China Meteorological Administration. It is a gridded dataset with 0.25° spatial resolution and interpolated by station-based observations from more than 2000 gauge stations located across China. The precipitation is first interpolated by thin-plate smoothing splines and then a gridded daily anomaly derived from angular distance weighting method is added to climatology to obtain the final precipitation dataset.[52] Due to its higher spatial resolution and accuracy relative to other grided observations in China, the dataset has been widely used to verify the output of climate numeric simulations overChina.[53–55] The output of bias correction is remapped into the same resolution with observation for further analysis. The whole study domain and its subregions of China are shown in Figure S1 and Table S3.

Extreme precipitation indices

The ETCCDI extreme precipitation indices, which are defined by the Expert Team on Climate Change Detection and Indices[56] are applied in this study. There are 10 extreme precipitation indices in total. In view of their definitions, they are divided into intensive or frequency indices, plus an annual total precipitation index. In this paper, we mostly focus our attention on the very heavy precipitation extremes events, i.e., the total precipitation (PRCPTOT), two intensive indices (Rx5day and R99pTOT) and two frequent indices (R20mm and CWD). Specifically, the PRCPTOT depicts the overall precipitation changes. The Rx5day is the maximum consecutive 5-day precipitation. R20mm is the days of heavy precipitation when daily precipitation is more than 20mm. The maximum number of consecutive wet days when daily precipitation is more than 1mm is defined as the CWD. The R99pTOT represents very heavy precipitation. The Rx5day and R99pTOT are the intensive indices and R20mm and CWD represent the frequency indices of precipitation-related extreme events. The detailed equations of five precipitation indices are shown in our supplementary materials (see Table S4).

Quantification of the avoided impacts

In addition, the avoided impact of precipitation extremes at 1.5°C compared with the 2.0°C warming level is calculated using the formula below[49,57]:

$$AI = \frac{C_{2.0} - C_{1.5}}{C_{2.0}} \times 100\% \quad \text{(Equation 3)}$$

where AI is the avoided impact, $C_{2.0}$ and $C_{1.5}$ represent the changes of precipitation extreme indices at 2.0°C and 1.5°C global warming levels.

Similarly, relative to the SSP245 emission scenario, the avoided impact for SSP370 and SSP585 is computed using the formula as follows:

$$AI = \frac{C_{ssp370(585)} - C_{ssp245}}{C_{ssp370(585)}} \times 100\% \quad \text{(Equation 4)}$$